14th IEA Heat Pump Conference
15-18 May 2023, Chicago, Illinois

A modified effectiveness-based approach in performance prediction of simultaneous heat and mass transfer in heat pump operating conditions

Ruozhou Du[a], Jiabao An[a], Long Huang[a*]

[a]Xi'an Jiaotong-Liverpool University, 111 Ren'ai Road, Suzhou, P. R. China, 215123

Abstract

This paper provides a systematic review of mathematical models for simultaneous heat and mass transfer process modeling. Models were categorized into lumped models, zone models, and numerical methods with information on their computation costs and accuracies. Observing the reviewed models, it was revealed that iterative calculations and complicated analytical corrections on fin efficiency are necessary under fully wet conditions. To provide the explicit calculation for the dehumidification process for micro-channel heat exchangers, regression techniques, like Multiple Polynomial Regression, are applied to modify the effectiveness-NTU method. The improved regression models show advances in accuracy and usability within the common geometries and conditions for heat pump applications.

Selection and/or peer-review under the responsibility of the organizers of the 14th IEA Heat Pump Conference 2023.

Keywords: Microchannel Heat Exchanger; Dehumidification; Heat Pump; Modeling

1. Introduction

In recent years, the mathematical models for the pure heat transfer process in heat exchangers are well developed. Classic models like Logarithm Mean Temperature Difference (LMTD) method and the effectiveness-NTU method provide a reasonable level of accuracy under fully dry conditions. However, once dehumidification occurs in the cooling process, the prediction of simultaneous heat and mass transfer becomes complicated while both sensible and latent capacity needs to be calculated. For instance, the traditional LMTD method is unable to calculate the latent heat during the condensation of humid air. To properly model this dehumidification process, various modified models were proposed, which are worth a systematic review to foster further studies. Hence, this article comprehensively summarizes current mathematical models for the dehumidification process within heat exchangers in section 2. The review reveals that iterative calculation and complicated analytical correction on fin efficiencies are contained in most of those models to approach reasonable accuracy, which shows little practical usability for engineers. To tackle this problem, regression-based modified explicit models, for Microchannel Heat Exchangers (MCHXs), are proposed in section 3. Finally, the proposed regression models are assessed and compared with traditional methods in section 4.

2. Review of mathematical models

For the modeling of simultaneous heat and mass transfer processes, [1] and [2] summarized several methods for the dehumidifying process of fin-and-tube heat exchangers, providing comprehensive reviews on this topic. Further, [3] gives a general framework for the categorization of those models. The existing models for simultaneous heat and mass transfer prediction of heat exchangers could be generally classified into three types: the lumped model, distributed parameter model (multi-node/numerical model), and the zone model. The

* Corresponding Author. *E-mail address:* long.huang@xjtlu.edu.cn

lumped models compute the cooling performance based on the lumped parameters, with the advantage of fast calculation. However, the details of the mass transfer process, such as the wetting area along the fin, are not considered. To account for detailed heat and mass transfer processes and approach higher prediction accuracy, numerical models can be used. Those methods tend to compute the cooling capacity of heat exchangers cell by cell. Each cell is treated with lumped parameters. Nevertheless, those methods are usually computationally expensive and hence lack practicality for fast performance predictions. The zone model slots in between lumped models and numerical approaches in terms of accuracy and computational cost. Those approaches divide the heat exchangers into different portions. Each portion is considered a lumped model with distinctive working circumstances. With various partitioning procedures, the calculation accuracy would be improved compared with the overall lumped models, yet the time for computation is reasonable in terms of the numerical methods. Based on these categories, the mainstream methods would be further introduced in the following section.

2.1. Lumped models

Based on the formulation of different models, the lumped models could be further summarized into temperature difference-based, effectiveness-based, and enthalpy difference-based models.

2.1.1. Temperature difference-based models

All the temperature difference-based methods originate from the classic LMTD method. However, modifications have to be introduced since the above equation cannot predict the latent heat. According to [2], the simplest way to modify is by introducing an empirical factor. The empirical factor is expressed as

$$\xi = \frac{i_{a,i} - i_{a,o}}{C_{pa} \cdot \left(T_{a,i} - T_{a,o}\right)} \tag{1.}$$

The empirical factor transfers the temperature difference into the enthalpy difference to cover the evaluation of latent heat. Although this is a quick method, the empirical factor may vary along the dehumidification process and a large deviation may be caused by that. Concerning that, McQuiston [4] introduced the condensation factor into the overall heat transfer coefficient with a similar idea. The condensation factor is defined as

$$C_f = \frac{w_a - w_{sat,w}}{T_a - T_w} \tag{2.}$$

The essence of this modification is unifying the sensible heat term and latent heat term in the energy equation and expressing sensible and latent heat by temperature difference.

Several publications modify the temperature difference as well. To reduce the complexity brought by the condensation, the researchers transfer the dehumidification into the equivalent dry cooling process based on the constant enthalpy difference [5], which is named as Equivalent Dry-bulb Temperature (EDT) method. In detail, the dehumidification process 1-2 in the following figure is converted into the 1e-2e process, which owns the constant humidity ratio. The transfer process is shown in Figure 1.

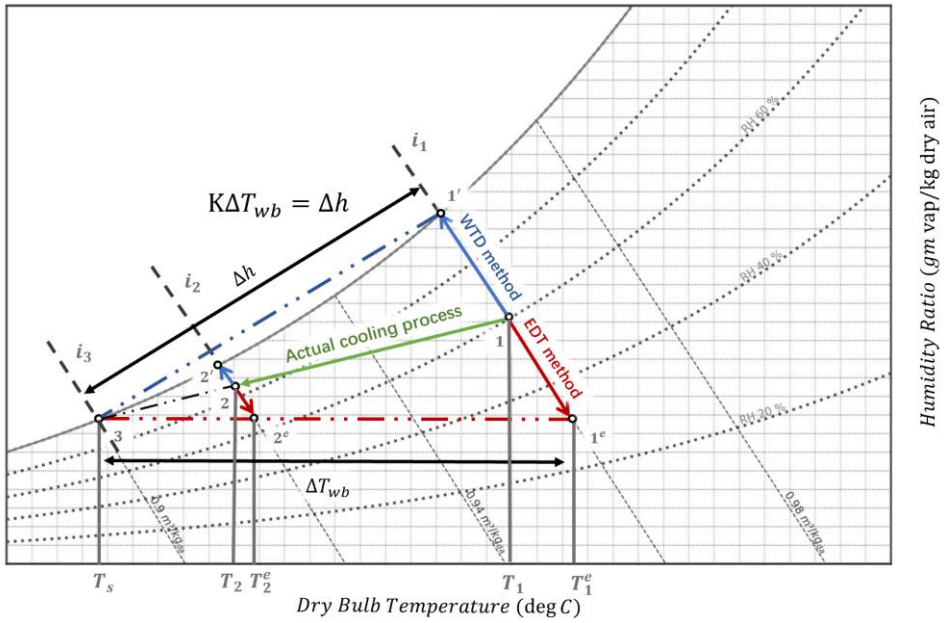

Figure 1 psychrometric charts for illustrating the assumptions of WTD method and the equivalent process of EDT method

Mathematically, the transformation of the heat transfer equation is

$$Q_t = \frac{h_{\text{wet}}A}{C_{\text{pa}}}\left(\frac{i_1 + i_2}{2} - i_{\text{w}}\right) = \frac{h_{\text{wet}}A}{C_{\text{pa}}}\left(\frac{i_1^e + i_2^e}{2} - i_{\text{w}}\right) \approx h_{\text{wet}}A\left(\frac{T_1^e + T_2^e}{2} - T_{\text{w}}\right) \quad (3.)$$

The other similar approach, namely Wet-bulb Temperature Difference (WTD) method [6]. This method was originally proposed for the indirect evaporative heat exchangers, aiming to transfer the enthalpy potential on the side of secondary air into the wet-bulb temperature difference. Considering point 1 in Figure 1 as the inlet of secondary air and point 2 as the outlet, those blue lines schematically exhibit this transformation. This method is based on two assumptions. The first is the linear variation assumption between saturated enthalpy difference and wet-bulb difference (shown as Eq.(4)).

$$K = \frac{\Delta i}{\Delta T_{wb}} \quad (4.)$$

The other one is assuming the lines 1' 2' and 1'3 in Figure 1 share the same value of K to simplify the derivation. Based on those two assumptions, the total heat transfer rate, for a parallel-flow configuration, is modified as

$$Q_t = U_{WTD}A\frac{\left(T_{pr}^{\text{i}} - T_{sc,wb}^{\text{i}}\right) - \left(T_{pr}^{\text{o}} - T_{sc,wb}^{\text{o}}\right)}{\ln\frac{T_{pr}^{\text{i}} - T_{sc,wb}^{\text{i}}}{T_{pr}^{\text{o}} - T_{sc,wb}^{o}}} \quad (5.)$$

Even though this approach is launched from air-to-air evaporators, the air-to-coolant heat exchangers could also use the same idea to rewrite the air-side transfer equation and re-derive Eq. (5) correspondingly.

2.1.2. Effectiveness-based models

As a classic predicting method, Braun[7] stated the effectiveness-NTU method for predicting fully dry conditions,

$$Q_d = \varepsilon_d \dot{m}_a C_{pa}\left(T_{a,i} - T_{w,i}\right) \quad (6.)$$

While under fully wet conditions, the total heat transfer rate is calculated by the enthalpy potential,

$$Q_t = \varepsilon_{wet}\dot{m}_a\left(i_{a,i} - i_{s,w,i}\right) \quad (7.)$$

The effectiveness in Eq. (6) and Eq. (7) is varied in different cases since it is a function of NTU, configurations of heat exchangers, etc. Hence, several basic derivations for effectiveness in different flow

arrangements under fully dry conditions are given by [8] and properly summarized in [9]. Additionally, to facilitate the use of effectiveness, some scholars also put efforts into simplifying the forms of effectiveness through a linear approximation between effectiveness and heat capacity rate ratio [10].

2.1.3. Enthalpy difference-based models

The classic LMED method for the dehumidifying condition was mentioned in several publications [11]–[13]. For instance, the cooling performance for Fin-and-Tube Heat Exchangers (FTHE), using LMED, is calculated as [2]

$$Q_t = U_{LMED} A_{total} \Delta i_{lm} \tag{8.}$$

$$\frac{1}{U_{LMED}} = \frac{b'_r A_t}{h_c A_{w,in}} + \frac{b'_p A_t \ln\left(\frac{D_{out}}{D_{in}}\right)}{2\pi k_w L_w} + \frac{A_t}{h_a \left(\frac{A_{w,in}}{b'_{w,p}} + \frac{\eta_{f,wet} A_f}{b'_{w,f}}\right)} \tag{9.}$$

The $b'_r, b'_p, b'_{w,p}, b'_{w,f}$represent the linear coefficients between saturated enthalpy differences and temperature differences, normally iterative calculations are needed to obtain accurate values. Detailed calculation procedures are given in [11]. According to Xia et al [14], the above LMED expression assumes the Lewis number as unity, which may cause deviations. Therefore, they fundamentally re-formulated the LMTD method to adapt the non-unity cases.

2.2. Zone models

As mentioned before, the zone models are mainly built on the concept of effectiveness and the major discrepancy is in the wet-dry boundary identification. For instance, [15] re-derived the correlations of effectiveness and NTU for counter-flow DX evaporators. The new correlations are integrated into the dry or wet area under partially wet conditions. Therefore, with the additional constraint from the dew point temperature of inlet air when computing the position of the boundary, the equation set can be closed and the areas of wet and dry could be obtained using those re-derived correlations.

Except for the above methods, another proposed explicit zone model is called Equivalent-Capacitance Approach (ECA) [16]. They found an alternative form for the LTMD method and it could avoid iterative calculation without introducing any further assumptions. Utilizing explicit expressions, they considered the two critical conditions, the just-dry-condition and the just-wet condition for coiling coils [17]. With the energy balances and the assumption of the surface temperature at the boundary is equivalent to the dew point temperature of inlet air, the critical coolant temperatures could be obtained. Comparing the two critical inlet refrigerant temperatures at just-dry-condition and just-wet-condition with actual inlet coolant temperature, the coil could be explicitly decided whether it is the fully wet, partially wet, or fully dry mode. Meanwhile, to partition the dry region into partially wet conditions, they formed an empirical correlation to maintain the explicit calculation.

Except for segmenting the heat exchangers from the airside, due to the phase change of the coolant, some publications proposed methods to separate the sub-cooling, saturation, and superheated regions on the refrigerant side. [18] developed the explicit methods of identifying those three portions through the calculation of volume fraction corresponding to the condensers, evaporators, and air coolers. In addition, [19] further divided the saturation region into region 1 and region 2, which was decided from the experiments. With the other two regions, the paper suggests a separate calculation for each portion through the effectiveness-NTU method and energy conservation equations and iteratively repeats the calculation process until the entire system meets the energy balance.

2.3. Numerical models

The numerical methods indicate the procedure that divides the heat exchangers into a large number of small cells and calculates them independently with basic governing equations. The numerical methods own high flexibility and accuracy on simulations, with the drawback of high computational expense. However, some numerical models would introduce some lumped parameters, such as the fin efficiency, to reduce the calculation time while maintaining reasonable accuracy, which is summarized as the semi-numerical models.

2.3.1. Semi-numerical models

The semi-numerical models introduced in this section indicate the methods that separate the entire heat exchangers into various segments and each segment could be considered as a small independent heat exchanger and is evaluated by lumped parameters. One representative semi-numerical model would be the Finite-Circular Fin Method (FCFM). FCFM originated from [20], they tend to evaluate the dehumidifying process of fin-and-tube heat exchangers segment-by-segment and each segment is equivalently considered as a fraction of a coil with a circular fin. The cooling performance is calculated by lumped LMED method, mentioned in section 2.1.2.

Consequently, they extend this method into the fully dry condition [21]. Distinguishing from the fully wet mode, the actual temperature difference is used. Noticing that the fin efficiency used in FCFM for the equivalent circular fin is derived in [22], for both fully dry and fully wet circumstances. In 2008, they added the evaluation to the partially wet condition using FCFM [23], a complicated analytical circular fin efficiency for partially wet conditions formulated by them. Later, as a comparison, FCFM was combined with the aforementioned EDT method to perform the calculation [24]. It was found that the FCFM based on the EDT method shows higher heat and mass transfer characteristics.

[25] also proposed the element-based approach according to the effectiveness-NTU method. It divides the cross-flow heat exchangers into many tiny elements. Each element is calculated independently. This discretizing method would provide higher simulation flexibility compared with the FCFM method.

2.3.2. Numerical models

To eliminate the use of fin efficiency in semi-numerical models, the grids on the fins are generated and each grid is calculated by basic governing equations. Based on this concept, a straightforward numerical method, named as Semi-explicit Method for Wall Temperature Linked Equations (SEWTLE), is proposed [26]. To provide a general numerical approach for any heat exchangers with complex geometry, this method focuses on describing the heat transfer during fluid cells (air cells or refrigerant cells) and wall cells (fin cells or tube wall cells). The governing equations are

$$\dot{m}_{flu} C_{p,flu} dT_{flu} = \sum_{j=1}^{\mathrm{n}} U_{local} \left(T_{\mathrm{w,cell}} - T_f\right) dA_{cell} \qquad (10.)$$

n represents the number of wall cells surrounding the fluid cells. The heat conduction along the wall cells by the two-dimension Laplace equation

$$\nabla\left(k_{local} t_{local} \nabla T_{\mathrm{w,cell}}\right) + \sum_{i=1}^{2} U_{local} \left(T_{\mathrm{w,cell}} - T_f\right) dA_{cell} = 0 \qquad (11.)$$

Eq. (10) could solve the fluid temperatures based on adjacent wall cell temperatures and Eq. (11) could obtain the wall cell temperatures based on neighboring temperatures of wall cells and fluid cells. Therefore, an iterative calculation would be performed once initial guess values are given to wall cells.

However, the mass transfer prediction for the dehumidifying condition was missed in SEWTLE. Therefore, [27] extend the application range of the original SEWTLE method into the fully wet condition and re-named it Fin2D-W. Further, the superheated region on the coolant side was also concerned in later research [28]. However, due to the heavy computation issue of this method, they applied the Fin theory on the fin cells to ease the computation process and therefore developed a new model called Fin2B-MB [29]. According to the authors, the introduction of fin theories would make the model overpredict the latent heat transfer rate by about 2%, and underpredict the sensible heat transfer rate by 4%.

Another constraint of the SEWTLE is its inconvenience in evaluating the irregular geometry boundary, such as the edge of holes on the fin. To improve the model feasibility on this issue, [30] mentioned a 2D model, which introduced several coefficients for irregular grids and changed the discretizing form of the 2D Laplace equation, making it could express irregular grids at boundaries.

3. Regression model development

Except for those models derived from classic methods, statistical tools also could be used for the predictions of the thermal behavior of heat exchangers. According to [31], serval types of techniques are widely applied for the statistical modeling of cooling systems, including the Artificial Neuron Network (ANN), Genetic Programming (GA), Multiple Linear Regression (MPR), etc. [32] specifically pointed out the basic regression

analysis that can be used, such as the linear/nonlinear regression, the multiple polynomial regression, and the stepwise regression, etc. Further, they gave a representative example of utilizing the MPR analysis on the cooling system. In this case, to maintain acceptable model accuracy, they chose the 8th degree during the regression, which causes 494 terms in the model. It is believed that the usability of this model is reduced by the enormous amount of terms. As a comparison, several studies developed regression models with fewer terms, yet fewer input variables [33]–[35]. In regard, another type of strategy to perform the regression is integrating heat transfer equations. For instance, combining several basic governing equations in non-dimensional forms, [36] proposed simpler performance correlations for indirect evaporative heat exchangers, expressed by Eq. (12).

$$\mathrm{T_{c,o}} = \psi \cdot \Pi_1^a \cdot \Pi_2^b \cdot \Pi_3^c \tag{12}$$

ψ, a, b, c are empirical coefficients and Π_1, Π_2, Π_3 are the derived dimensionless parameters.

This type of methodology can be also utilized in the present study. In Section 2, it becomes evident that the majority of dehumidification models require iterative calculations, which increases the computational load for real-time simulation of thermodynamic cycle systems. Additionally, the fin efficiency, which is formulated based on rectangular fin geometry, cannot perfectly suit MCHX due to the assumption of the adiabatic boundary at the middle height of the fin. As result, it causes a deviation in the prediction of heat capacity under both fully wet and dry conditions. To address the raised computational load in fully wet conditions and the accuracy limitations brought about by analytical fin efficiency, a regression-based modification has been made to the explicit effectiveness model under fully wet/dry conditions for two-phase refrigerant in this section. The regression is based on the dataset generated by the numerical model Fin2D-W mentioned in section 2.3.2. The explicit effectiveness-based models for the fully wet and dry conditions are stated in section 3.1 and section 3.2 respectively. In section 3.3, the selected regression variables and corresponding ranges are described to elaborate on the application range of the proposed model.

3.1. Explicit model for fully dry condition

For the pure heat transfer process of MCHX, the classic effectiveness-NTU model is used. With two-phase refrigerant, the effectiveness is described as

$$\varepsilon = 1 - \exp(-NTU_t) \tag{12.}$$

where

$$C_r = \frac{C_{min}}{C_{max}}$$

$$NTU_t = \frac{U_t A_t}{\dot{m}_a C_{pa}}$$

$$U_t = \frac{1}{\left(\frac{1}{h_c} + \frac{t_f}{k_w}\right)\left(\frac{A_t}{A_{f,t}}\right) + \frac{1}{\eta_{sf,d} h_a}}$$

The overall surface efficiency is calculated as

$$\eta_{sf,d} = 1 - \frac{A_{f,t}}{A_t}\left(1 - \eta_{f,d}\right) \tag{13.}$$

Therefore the Q_t is calculated by

$$Q_t = \varepsilon_d \dot{m}_a C_{pa}\left(T_{r,i} - T_{a,i}\right) \tag{14.}$$

To improve the prediction accuracy, efficiency is the regression objective so that the temperature profile along the fin can be better described within the selected variable ranges.

3.2. Explicit model for fully wet condition

To perform an explicit calculation procedure for fully wet conditions, the expression for total heat transfer rate is re-derived as Eq. (15).

$$Q_t = \varepsilon_m \dot{m}_a (i_{a,i} - i_{s,r}) \quad (15.)$$

where

$$\varepsilon_m = \frac{1}{\frac{1}{\varepsilon} + \frac{c_s \dot{m}_a}{\alpha_i A_i}}$$

$$\varepsilon = \left(1 - \exp\left(-\frac{\alpha_o \eta_{sf,wet} A_o}{\dot{m}_a C_{pa}}\right)\right)$$

$$\eta_{sf,wet} = 1 - \frac{A_{f,t}}{A_t}(1 - \eta_{f,wet})$$

$$c_s = \frac{(i_{sat,f} - i_{sat,r,i})}{(T_w - T_r)}$$

And the sensible heat transfer is obtained by Eq. (16).

$$Q_s = \left(1 - \exp\left(-\frac{\alpha_o \eta_{s,wet} A_o}{\dot{m}_a C_{pa}}\right)\right) \dot{m}_a C_{pa} (T_{a,i} - T_f) \quad (16.)$$

Naturally, to formulate the explicit calculation process, c_s has to be regressed based on the input parameters. To provide sufficiently accurate c_s, the MPR technique is selected. In addition, to describe the enthalpy profile and temperature profile more accurately, η_f used in Eq. (15) for the calculation of Q_t and η_f used in Eq. (16) for the calculation of Q_s are independently regressed. the regression results are exhibited in section 3.4. Overall, the explicit calculation procedure is **(i)** calculate the Q_t by Eq. (16), with regressed c_s and $\eta_{f,w}$ for total heat transfer rate, **(ii)** calculate the tube wall temperature by Eq. (17), **(iii)** lastly calculate the Q_s by Eq. (16), with the regressed fin efficiency $\eta_{f,w}$ for the calculation of Q_s.

$$T_w = \frac{Q_t}{h_c A_i} + T_{ref} \quad (17.)$$

3.3. Selection of variables and ranges

To cover most of the influential input variables, nine inputs are selected to design the experiments for dry conditions and ten variables for wet conditions. Selected variables include the mass flow rate of coolant $\dot{m}_r$, the air velocity v_a, the inlet air temperature $T_{a,i}$, the inlet refrigerant temperature $T_{r,i}$, the Relative humidity of inlet air RH, the fin depth L_f and the fin height H_f, the Air-side Heat Transfer Coefficient (AHTC), expressed by h_a, Refrigerant-side Heat Transfer Coefficient (RHTC), expressed by h_c and the half spacing of the MCHX is denoted as hs. All the selected variables are illustrated in Figure 2(a). The input variable RH is ignored under fully dry conditions.

Due to the substantial time cost of the Fin2D-W model, A 5-level 1/8 fractional factorial circumscribed Central Composite Design (CCD) is utilized to minimize the simulation time and optimize the regression results. The travel distance α between the axial point and central point is set at the value of 3.3636. 147 experiments are generated for dry condition simulation and 149 cases are generated for fully wet conditions. The relations between coded levels and actual levels, as well as selected input variables and corresponding ranges, are listed in Table 1. The value of the AHTC for each case is determined by the simple heat transfer correlation form provided by Wang and Chang [38], which is shown as

$$j = 0.425 Re_{Lp}^{-0.496} \quad (18.)$$

Since the prediction results of Eq. (18) are more moderate compared with the final equation in [38] and the correlation for plain fins provided by [39], meaning a wider range of fin geometry could be represented by the prediction. In terms of the RHTC, it is determined based on [40] for two-phase refrigeration flow boiling and based on [41] for condensing refrigerant flow. Moreover, to extend the range of AHTC and RHTC that contains in this regression, coefficients between 0.5-1.5 are multiplied before they are used in the calculation, which is

explained by Eq. (19) and (20). In other words, all the values of AHTC and RHTC randomly fluctuated by about ±50%. Those coefficients of AHTC and RHTC for cases are shown in Table 1.

$$h_c{}' = C_{RHTC} \times h_c \quad (19.)$$

$$h_a{}' = C_{AHTC} \times h_a \quad (20.)$$

Table 1. input variables and relations between coded level and actual level for CCD

General input variables						
Input variables	Unit	Five Coded levels				
		$-\alpha$	-1	0	1	α
$\dot{m}_r$	kg/s	3e-4	6.041e-4	1.05e-3	1.496e-3	1.8e-3
v_a	m/s	0.5	0.9054	1.5	2.0946	2.5
RH	$-$	0.4	0.5216	0.7	0.8784	1
L_f	m	0.015	0.017	0.02	0.023	0.025
H_f	m	0.008	0.0088	0.01	0.0112	0.0120
C_{RHTC}	$-$	0.5	0.7027	1	1.2973	1.5
C_{AHTC}	$-$	0.5	0.7027	1	1.2973	1.5
hs	m	1.1250e-4	1.8669e-4	2.9550e-4	4.0431e-4	4.7850e-4
Specified input temperatures for the fully wet condition with two-phase refrigerant						
$T_{r,i}$	K	277.15	278.37	280.15	281.93	283.15
$T_{a,i}$	K	293.15	295.18	298.15	301.12	303.15
Specified input temperatures for the fully dry condition with two-phase refrigerant						
$T_{r,i}$	K	323.15	327.20	333.15	339.10	343.15
$T_{a,i}$	K	303.15	305.18	308.15	311.12	313.15

Meanwhile, the test dataset, for the validation of regression models, is generated randomly within the ranges listed in Table 1. 24 cases for the test dataset are picked, as roughly 20% of the training dataset for both dry and fully wet conditions.

4. Result and discussion

In this section, the regression results are listed, and the performance concerning the calculation time and prediction accuracy are elaborated.

4.1. Regression results

(a) Fully wet conditions

The wet fin efficiency η_{Qt} used in the calculation of Q_t is obtained by Eq. (47)

$$\eta_{Qt} = \eta_{wet}^{\mu_1} \quad (21.)$$

where

$$\eta_{wet} = \frac{\tanh(mH_f)}{mH_f}$$

$$m = \sqrt{\frac{2.1493\alpha_o}{k_w t_f}}$$

$$\mu_1 = 1.7290\xi_1 + 0.2301\xi_1^2$$

$$\xi_1 = \left(\frac{\alpha_o}{\alpha_i}\right)^{0.0365}\left(\frac{H_f}{L_f}\right)^{-0.1418}\left(\frac{hs}{L_f}\right)^{0.1594}\left(\frac{T_{a,i}}{T_r}\right)^{-0.3249}\left(\frac{\rho_a V_a H_f hs}{\dot{m}_r}\right)^{-0.0331}(RH)^{0.0983}$$

It should be noted that the regression basis η_{wet}, which pertains to fully wet conditions, maintains a similar form to the analytical solution under dry conditions due to its superior predictive performance when compared to other forms. In terms of the wet fin efficiency used in the calculation of Q_s,

$$\eta_{Qs} = \eta_{wet}^{\mu_2} \tag{22.}$$

where

$$\mu_2 = -0.8904\xi_2 + 2.2120\xi_2^2$$

$$\xi_2 = \left(\frac{H_f}{L_f}\right)^{-0.0921}\left(\frac{hs}{L_f}\right)^{0.0742}\left(\frac{T_{a,i}}{T_r}\right)^{2.2396}\left(\frac{\rho_a V_a H_f hs}{\dot{m}_r}\right)^{-0.0138}(RH)^{0.2792}$$

The regression results of c_s that are regressed in the form of MPR are exhibited in the Appendix.

(b) Fully dry conditions

The analytical dry efficiency expression is still maintained as Eq. (23).

$$\eta_d = \frac{\tanh\left(\frac{mH_f}{2}\right)}{\frac{mH_f}{2}} \tag{23.}$$

$$m = \sqrt{\frac{2\alpha_o}{k_w t_f}}$$

Yet the modified fin efficiency for the single-phase refrigerant is shown as

$$\eta_{m,d} = \eta_d^{\mu_3} \tag{24.}$$

Meanwhile, the modifications that apply to the two-phase flow are exhibited as follows.

$$\mu_3 = 1.9307\xi_2 + 2.2470\xi_2^2 \tag{25.}$$

where

$$\xi_3 = \left(\frac{\alpha_o}{\alpha_i}\right)^{0.0670}\left(\frac{H_f}{L_f}\right)^{-0.3489}\left(\frac{hs}{L_f}\right)^{0.1753}\left(\frac{T_{a,i}}{T_r}\right)^{1.4307}\left(\frac{\rho_a V_a H_f hs}{\dot{m}_r}\right)^{-0.1094}$$

4.2. Model assessment

The prediction performance is assessed based on two indexes, the Mean Absolute Error (MAE) and Maximum Error (ME) of training/test datasets, which are shown in Eq. (25) and (26). The performances are exhibited in Tables 2 and 3 for fully dry and fully wet conditions accordingly. Note that the single potential effectiveness-NTU model is used, which is stated in [33].

$$\text{MAE} = MEAN\left(\frac{\left|Q_{num,i} - Q_i\right|}{Q_{num,i}}\right) \tag{26.}$$

$$\text{ME} = MAX\left(\frac{\left|Q_{num,i} - Q_i\right|}{Q_{num,i}}\right) \tag{27.}$$

Based on the test results presented in Table 2, it is evident that the developed regression model exhibits advance in prediction accuracy for two-phase flow conditions. The MAE and ME are improved by 0.1% and 0.3%, respectively. The developed model also shows superior prediction accuracy for dehumidification processes in two-phase refrigerant conditions. For the three types of heat transfer rates, the developed model

shows the advances at both MAE and ME, where the prediction of the sensible heat transfer rate is improved the most. For the sensible heat transfer rate, the MAE is reduced by about 1.2%, while the ME is improved by about 3%.

Furthermore, the developed model exhibits a faster computational process compared to iterative effectiveness-NTU, as shown in Table 4. In a nutshell, the present model is roughly 3 times quicker on average in two-phase refrigerant conditions for calculating one case, compared to effectiveness-NTU. The data presented in Table 4 is gained from the first hundred cases in the training datasets.

Table 2 performances of models in the test dataset under fully dry condition

Models	Two-phase (24 cases)	
	MAE (%)	ME (%)
Present model	0.74	1.99
Effectiveness-NTU	0.88	2.35

Table 3 performances of models in test dataset under fully wet condition

Models		Two-phase (24 cases)	
		MAE (%)	ME (%)
Present model	Q_t	0.54	1.44
	Q_s	0.47	1.13
	Q_l	0.72	2.27
Effectiveness-NTU	Q_t	0.95	3.36
	Q_s	1.69	4.34
	Q_l	0.99	4.88

Table 4 calculation time comparison of models

		Fully wet with two-phase (s)
Present model	Max time	2.4e-3
	Average time	1.3e-3
Effectiveness-NTU	Max time	1.1e-2
	Average time	4.6e-3
Numerical Fin2D-W	Max time	2.22e+3
	Average time	4.09e+2

5. Conclusions

This paper systematically reviews the mathematical models for the prediction of the dehumidification process. Three types of models are classified, and each has its characteristics of computational cost and accuracy. Based on the review models, it is found that most models in wet conditions require iteration computations and complicated correction on fin efficiency based on various geometries. To improve the usability of dehumidification prediction models, fully wet and fully dry explicit models for two-phase refrigerants are proposed based on the analytical effectiveness-NTU method. The regressions are carried out in a wide range of air and refrigerant side conditions, as well as commonly used geometric parameter ranges. Three main advantages of the proposed models are the explicit calculation for dehumidification calculation with improved accuracy as compared with traditional lumped models.

The research carried out here should benefit the academic and engineering communities with the need to conduct fast heat and mass transfer analysis for MCHX in heat pump applications. The regression methods presented here can be employed in the future as part of heat exchanger optimization studies for a wider range of conditions and geometries.

Nomenclature

A	area [m^2]	k	thermal conductivity
b'_p	slope of the air saturation curve between the outside and inside tube wall temperature	ζ_2	regression coefficient for fin efficiency modification
b'_r	slope of the air saturation curve between the mean water temperature and the inside wall temperature	$\dot{m}$	mass flow rate of air [Kg/s]
$b'_{w,f}$	slope of the saturated moist air enthalpy curve at the mean water film temperature of fin surface	L_w	tube length
$b'_{w,p}$	slope of the saturated moist air enthalpy curve at the mean water film temperature of pipe outer-wall surface	L_f	fin depth, exhibit in Figure 2.
C_f	condensation factor [Kg/K]	L_p	louver pitch
C_{pa}	air specific heat capacity [KJ/kg/K]	n	the number of wall cells surrounding the fluid cells
C_s	rate of change of the specific enthalpy with temperature along the saturated air line [kJ kg-1 K-1]	NTU	Heat transfer unit
C_r	Heat Capacity Ratio	Q	heat transfer rate [KJ/Kg]
D	tube diameter	Re_{Lp}	Reynolds number based on louver pitch, defined by $G * L_p/\nu$
H_f	fin height, exhibit in Figure 2.	RH	relative humidity of the inlet air, exhibit in Figure 2
hs	half spacing of the fin, exhibit in Figure 2	T	temperature [K]
h	heat transfer coefficient [W m−2 K−1]	t	fin thickness [m]
i	enthalpy [KJ]	U	overall heat transfer coefficient [W m−2 K−1]
j	the Colburn factor	ν	viscosity [Pa s]
K	slope defined by Eq. (4)	v_a	Velocity of the air [m s-1]
β	parameter defined by Eq. (22)	w	humidity ratio [Kg]
γ	regression coefficient for dry condition modification, defined by Eq. (19)	η	Surface or fin efficiency
ε	effectiveness	ξ	empirical factor [-]

Subscript	Description	**Subscript**	Description
$AHTC$	air-side heat transfer coefficient	$RHTC$	refrigerant-side heat transfer coefficient
a	air	c	coolant
cell	at this cell	**s**	sensible
d	dry	sat	saturated
f	fin	sc	secondary air for indirective evaporators

flu	at a Fluid cell	t	total
i	inlet	WTD	for wet-bulb temperature difference method
in	inside	w	wall
$local$	at local position	wb	wet-bulb
o	outlet	$\mathbf{wet}$	under wet condition
out	outside	$\mathbf{1}$	inlet
pr	primary air for indirective evaporators	$\mathbf{2}$	outlet
sf	surface		

Superscript	Description
e	element
$\mathbf{i}$	inlet
$\mathbf{o}$	outlet

Acknowledgements

This work was supported by the Natural Science Foundation of the Higher Education Institutions of Jiangsu Province, China (Grant No. 21KJB470011), State Key Laboratory of Air-conditioning Equipment and System Energy Conservation Open Project (Project No. ACSKL2021KT01) and the Xi'an Jiaotong-Liverpool University Research Development Fund (RDF 20-01-16).

References

[1] W. Pirompugd, C. C. Wang, and S. Wongwises, "A review on reduction method for heat and mass transfer characteristics of fin-and-tube heat exchangers under dehumidifying conditions," *International Journal of Heat and Mass Transfer*, vol. 52, no. 9–10, pp. 2370–2378, Apr. 2009, doi: 10.1016/j.ijheatmasstransfer.2008.10.019.

[2] G. Zhang, B. Wang, X. Li, W. Shi, and Y. Cao, "Review of experimentation and modelling of heat and mass transfer performance of fin-and-tube heat exchangers with dehumidification," *Applied Thermal Engineering*, vol. 146. Elsevier Ltd, pp. 701–717, Jan. 05, 2019. doi: 10.1016/j.applthermaleng.2018.10.032.

[3] G. liang Ding, "Recent developments in simulation techniques for vapour-compression refrigeration systems," *International Journal of Refrigeration*, vol. 30, no. 7. pp. 1119–1133, Nov. 2007. doi: 10.1016/j.ijrefrig.2007.02.001.

[4] F. C. Mcquiston, "Fin efficiency with combined heat and mass transfer," 1975.

[5] J. Wang and E. Hihara, "Prediction of air coil performance under partially wet and totally wet cooling conditions using equivalent dry-bulb temperature method," 2003. [Online]. Available: www.elsevier.com/locate/ijrefrig

[6] X. Cui, K. J. Chua, M. R. Islam, and W. M. Yang, "Fundamental formulation of a modified LMTD method to study indirect evaporative heat exchangers," *Energy Conversion and Management*, vol. 88, pp. 372–381, 2014, doi: 10.1016/j.enconman.2014.08.056.

[7] J. E. Braun, S. A. Klein, and J. W. Mitchell, "Effectiveness models for cooling tower and cooling coils," 1989.

[8] D. Taler, *Numerical Modelling and Experimental Testing of Heat Exchangers*, vol. Volume 161. Polish Academy of Sciences, 2019. [Online]. Available: http://www.springer.com/series/13304

[9] G. Zhou, Y. Ye, W. Zuo, X. Zhou, and X. Wu, "Fast and efficient prediction of finned-tube heat exchanger performance using wet-dry transformation method with nominal data," *Applied Thermal Engineering*, vol. 145, pp. 133–146, Dec. 2018, doi: 10.1016/j.applthermaleng.2018.09.020.

[10] R. Laskowski, "The concept of a new approximate relation for exchanger heat transfer effectiveness for a cross-flow heat exchanger with unmixed fluids. *Journal of Power Technologies* 91 (2) (2011) 93-101 The concept of a new approximate relation for exchanger heat transfer effectiveness for a cross-flow heat exchanger with unmixed fluids." [Online]. Available:

https://www.researchgate.net/publication/266289611
[11] C.-C. Wang, Y.-C. Hsieh, and Y.-T. Lin, "Performance of Plate Finned Tube Heat Exchangers Under Dehumidifying Conditions," 1997. [Online]. Available: http://heattransfer.asmedigitalcollection.asme.org/
[12] X. Ma, G. Ding, Y. Zhang, and K. Wang, "Airside characteristics of heat, mass transfer and pressure drop for heat exchangers of tube-in hydrophilic coating wavy fin under dehumidifying conditions," *International Journal of Heat and Mass Transfer*, vol. 52, no. 19–20, pp. 4358–4370, Sep. 2009, doi: 10.1016/j.ijheatmasstransfer.2009.03.066.
[13] Q. Liu, J. Liu, L. Zhang, and X. Xu, "Effect of environmental pressure on heat and mass transfer characteristics for fin-and-tube heat exchangers under non-unit Lewis factor," *Applied Thermal Engineering*, vol. 116, pp. 784–791, 2017, doi: 10.1016/j.applthermaleng.2017.01.093.
[14] L. Xia, M. Y. Chan, S. M. Deng, and X. G. Xu, "A modified logarithmic mean enthalpy difference (LMED) method for evaluating the total heat transfer rate of a wet cooling coil under both unit and non-unit Lewis Factors," *International Journal of Thermal Sciences*, vol. 48, no. 11, pp. 2159–2164, Nov. 2009, doi: 10.1016/j.ijthermalsci.2009.04.002.
[15] M. K. Mansour and M. A. Hassab, "Novel lumped modelling for determining thermal performance of DX evaporator under partially-wet and fully-wet conditions," *Applied Thermal Engineering*, vol. 98, pp. 1025–1035, Apr. 2016, doi: 10.1016/j.applthermaleng.2015.12.094.
[16] C. K. Lee and H. Nam, "An equivalent-capacitance approach for determining the performance of a refrigerant coil," in *Progress in Sustainable Energy Technologies Vol II: Creating Sustainable Development*, Springer International Publishing, 2014, pp. 421–429. doi: 10.1007/978-3-319-07977-6_28.
[17] C. K. Lee, "A simplified explicit model for determining the performance of a chilled water cooling coil," *International Journal of Refrigeration*, vol. 43, pp. 167–175, 2014, doi: 10.1016/j.ijrefrig.2014.04.003.
[18] C. K. Lee and H. N. Lam, "Simplified explicit calculation algorithms for determining the performance of refrigerant coils in vapour-compression systems," *International Journal of Refrigeration*, vol. 38, no. 1, pp. 178–188, Feb. 2014, doi: 10.1016/j.ijrefrig.2013.08.023.
[19] Y. T. Ge and R. Cropper, "Performance evaluations of air-cooled condensers using pure and mixture refrigerants by four-section lumped modelling methods," *Applied Thermal Engineering*, vol. 25, no. 10, pp. 1549–1564, Jul. 2005, doi: 10.1016/j.applthermaleng.2004.10.001.
[20] W. Pirompugd, S. Wongwises, and C. C. Wang, "A tube-by-tube reduction method for simultaneous heat and mass transfer characteristics for plain fin-and-tube heat exchangers in dehumidifying conditions," *Heat and Mass Transfer*, vol. 41, no. 8, pp. 756–765, Jun. 2005, doi: 10.1007/s00231-004-0581-x.
[21] W. Pirompugd, C. C. Wang, and S. Wongwises, "A fully wet and fully dry tiny circular fin method for heat and mass transfer characteristics for plain fin-and-tube heat exchangers under dehumidifying conditions," *J Heat Transfer*, vol. 129, no. 9, pp. 1256–1267, Sep. 2007, doi: 10.1115/1.2739589.
[22] K. T. Hong and R. L. Webb, "Calculation of fin efficiency for wet and dry fins," *HVAC and R Research*, vol. 2, no. 1, pp. 27–41, 1996, doi: 10.1080/10789669.1996.10391331.
[23] W. Pirompugd, C. C. Wang, and S. Wongwises, "Finite circular fin method for wavy fin-and-tube heat exchangers under fully and partially wet surface conditions," *International Journal of Heat and Mass Transfer*, vol. 51, no. 15–16, pp. 4002–4017, Jul. 2008, doi: 10.1016/j.ijheatmasstransfer.2007.11.049.
[24] W. Pirompugd, C. C. Wang, and S. Wongwises, "The New Mathematical Models for Plain Fin-and-Tube Heat Exchangers with Dehumidification," *Journal of Heat Transfer*, vol. 137, no. 3, Mar. 2015, doi: 10.1115/1.4029037.
[25] H. A. Navarro and L. C. Cabezas-Gómez, "Effectiveness-NTU computation with a mathematical model for cross-flow heat exchangers," vol. 24, no. 04, pp. 509–521, [Online]. Available: www.abeq.org.br/bjche
[26] J. M. Corberán, P. F. de Córdoba, J. Gonzálvez, and F. Alias, "Semiexplicit method for wall temperature linked equations (SEWTLE): A general finite-volume technique for the calculation of complex heat exchangers," *Numerical Heat Transfer, Part B: Fundamentals*, vol. 40, no. 1, pp. 37–59, Jul. 2001, doi: 10.1080/104077901300233596.
[27] A. H. Hassan, S. Martinez-Ballester, and J. Gonzalvez-Macia, "A comparative study between a two-dimensional numerical minichannel evaporator model and a classical effectiveness–NTU approach under different dehumidifying conditions," *Science and Technology for the Built Environment*, vol. 21, no. 5, pp. 681–692, 2015, doi: 10.1080/23744731.2015.1028866.
[28] A. Hussein Hassan, S. Martínez-Ballester, and J. Gonzálvez-Maciá, "Two-dimensional numerical modelling for the air-side of minichannel evaporators accounting for partial dehumidification

scenarios and tube-to-tube heat conduction," *International Journal of Refrigeration*, vol. 67, pp. 90–101, Jul. 2016, doi: 10.1016/j.ijrefrig.2016.04.003.

[29] A. H. Hassan, S. Martínez-Ballester, and J. Gonzálvez-Maciá, "A new moving boundary model for evaluating the performance of wet fins: Application to minichannel evaporators," *Applied Thermal Engineering*, vol. 127, pp. 566–579, Dec. 2017, doi: 10.1016/j.applthermaleng.2017.08.055.

[30] S. Y. Liang, T. N. Wong, and G. K. Nathan, "Comparison of one-dimensional and two-dimensional models for wet-surface efficiency of a plate-and-tube heat exchanger." [Online]. Available: www.elsevier.com/locate/apthermeng

[31] A. Sohani, H. Sayyaadi, H. Hasani Balyani, and S. Hoseinpoori, "A novel approach using predictive models for performance analysis of desiccant enhanced evaporative cooling systems," *Applied Thermal Engineering*, vol. 107, pp. 227–252, Aug. 2016, doi: 10.1016/j.applthermaleng.2016.06.121.

[32] Y. G. Akhlaghi, X. Ma, X. Zhao, S. Shittu, and J. Li, "A statistical model for dew point air cooler based on the multiple polynomial regression approach," *Energy*, vol. 181, pp. 868–881, Aug. 2019, doi: 10.1016/j.energy.2019.05.213.

[33] F. Comino, S. Milani, S. de Antonellis, C. M. Joppolo, and M. Ruiz de Adana, "Simplified performance correlation of an indirect evaporative cooling system: Development and validation," *International Journal of Refrigeration*, vol. 88, pp. 307–317, Apr. 2018, doi: 10.1016/j.ijrefrig.2018.02.002.

[34] A. Pakari and S. Ghani, "Regression models for performance prediction of counter flow dew point evaporative cooling systems," *Energy Convers Management*, vol. 185, pp. 562–573, Apr. 2019, doi: 10.1016/j.enconman.2019.02.025.

[35] D. Pandelidis and S. Anisimov, "Application of a statistical design for analyzing basic performance characteristics of the cross-flow Maisotsenko cycle heat exchanger," *International Journal of Heat and Mass Transfer*, vol. 95, pp. 45–61, Apr. 2016, doi: 10.1016/j.ijheatmasstransfer.2015.11.060.

[36] X. Cui, M. R. Islam, B. Mohan, and K. J. Chua, "Developing a performance correlation for counter-flow regenerative indirect evaporative heat exchangers with experimental validation," *Applied Thermal Engineering*, vol. 108, pp. 774–784, Sep. 2016, doi: 10.1016/j.applthermaleng.2016.07.189.

[37] W. Pirompugd and S. Wongwises, "Partially wet fin efficiency for the longitudinal fins of rectangular, triangular, concave parabolic, and convex parabolic profiles," *Journal of the Franklin Institute*, vol. 350, no. 6, pp. 1424–1442, Aug. 2013, doi: 10.1016/j.jfranklin.2013.02.019.

[38] Y.-J. Chang and C.-C. Wang, "A generalized heat transfer correlation for louver fin geometry," 1997.

[39] P. Teertstra, M. M. Yovanovich, J. H. Culham, and T. Lemczyk, "Analytical forced convection modeling of plate fin heat sinks," *Annual IEEE Semiconductor Thermal Measurement and Management Symposium*, pp. 34–41, 1999, doi: 10.1109/stherm.1999.762426.

[40] M. M. Shah, "New general correlation for heat transfer during saturated boiling in mini and macro channels," *International Journal of Refrigeration*, vol. 137, pp. 103–116, May 2022, doi: 10.1016/j.ijrefrig.2022.02.019.

[41] M. M. Shah, "A correlation for heat transfer during condensation in horizontal mini/micro channels," *International Journal of Refrigeration*, vol. 64, pp. 187–202, Apr. 2016, doi: 10.1016/j.ijrefrig.2015.12.008.

Appendix

C_s for Two-phase refrigerant under fully wet condition

Regression items	Coefficients
hs	773.3503278912
α_i	0.0000948948
L_f	38.3773722823
RH	−2.0216861869
$T_{r,i}$	−1.0152934629
$T_{a,i}$	−0.0558427117
v_a	−0.4891876154
$\dot{m}_r$	−5723.4507277779
$\alpha_i \times hs$	0.0024117767
α_i^2	0.0000000003
$\alpha_o \times hs$	0.6156383647
$\alpha_o \times \alpha_i$	−0.0000000170
$\alpha_i \times H_f$	−0.0001363495
$\alpha_o \times H_f$	0.0181053785
$L_f \times H_f$	3471.1090492644
$\alpha_i \times RH$	−0.0000059242
$\alpha_o \times RH$	0.0003096243
$RH \times L_f$	−2.0289842690
$\alpha_o \times T_{r,i}$	−0.0000155251
$RH \times T_{r,i}$	0.0033981273
$T_{r,i}^2$	0.0018169769
$T_{a,i} \times hs$	−2.7568565683
$\alpha_i \times T_{a,i}$	−0.0000003349
$\alpha_o \times T_{a,i}$	0.0000134885
$T_{a,i} \times H_f$	0.0131479250
$T_{a,i} \times L_f$	−0.1332461658
$RH \times T_{a,i}$	0.0040033968
$T_{a,i} \times T_{r,i}$	0.0002142941
$hs \times v_a$	−48.2247161957
$\alpha_i \times v_a$	−0.0000016500
$\alpha_o \times v_a$	0.0000684268
$L_f \times v_a$	−0.5824816663
$RH \times v_a$	0.0244457612
$T_{a,i} \times v_a$	0.0018222308
v_a^2	−0.0041959005
$\alpha_i \times \dot{m}_r$	0.0243469441
$T_{r,i} \times \dot{m}_r$	19.4632217323